Numerical analysis of superconducting phases in the extended Hubbard model with non-local pairing

University of Pisa, a.y. 2025-2026

Alessandro Gori*

Thesis for the Master's degree in Physics

Abstract

[To be continued...]

Contents

Draft: August 20, 2025

*a.gori23@studenti.unipi.it / nepero27178@github.com

List of symbols and abbreviations

AF	Anti-Ferromagnetic
BCS	Bardeen-Cooper-Schrieffer (theory)
DoF	Degree of Freedom
HF	Hartree-Fock
MFT	Mean-Field Theory
SC	Superconductor
T_c	Critical temperature

Introduction

This thesis project is about my favorite ice cream flavor. [To be continued...]

Chapter 1

Theoretical introduction

[To be continued...]

1.1 Antiferromagnetic ordering in the Hubbard model

Consider the ordinary Hubbard model:

$$\hat{H} = -t \sum_{\langle ij \rangle} \sum_{\sigma} \hat{c}^{\dagger}_{i\sigma} \hat{c}_{j\sigma} + U \sum_{i} \hat{n}_{i\uparrow} \hat{n}_{i\downarrow} \qquad t, U > 0 \tag{1.1}$$

The two competing mechanisms are site-hopping of amplitude t and local repulsion of amplitude U. For this model defined **on a bipartite lattice at half filling** and fixed electron number, it is well known [6] that, below a certain critical temperature T_c and above some (small) critical repulsion U_c/t, the ground-state acquires antiferromagnetic (AF) long-range ordering. schematically depicted in Fig. 1.1a. The mechanism for the formation of the AF phase takes advantage of virtual hopping, as described in App. **??**; the Mean-Field Theory (MFT) treatment of ferromagnetic-antiferromagnetic orderings in 2D Hubbard lattices is discussed in App. **??**.

In this chapter the discussion is limited to the two-dimensional square lattice Hubbard model. The lattice considered has L_ℓ sites on side $\ell = x, y$, thus a total of $L_x L_y$ sites. The total number of single electron states is given by $D = 2L_x L_y$. All theoretical discussion neglects border effects, thus considering $D \to +\infty$.

1.2 The Extended Fermi-Hubbard model

The Extended Fermi-Hubbard model is defined by:

$$\hat{H} = -t \sum_{\langle ij \rangle} \sum_{\sigma} \hat{c}^{\dagger}_{i\sigma} \hat{c}_{j\sigma} + U \sum_{i} \hat{n}_{i\uparrow} \hat{n}_{i\downarrow} - V \sum_{\langle ij \rangle} \sum_{\sigma\sigma'} \hat{n}_{i\sigma} \hat{n}_{j\sigma'} \tag{1.2}$$

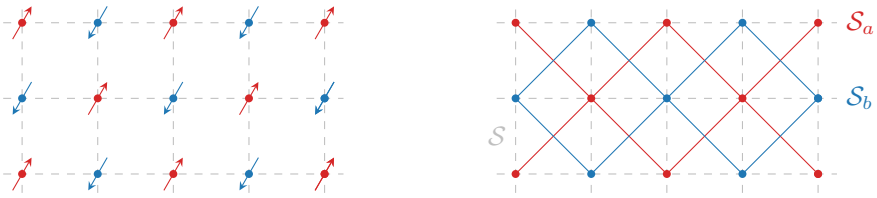

a | Antiferromagnetic phase. b | Polarized sublattices.

Figure 1.1 | Schematic representation of the AF phase. Fig. 1.1a shows a portion of the square lattice with explicit representation of the spin for each site. Fig. 1.1b divides the square lattice $\mathcal{S}$ in two polarized sublattices $\mathcal{S}_a$, $\mathcal{S}_b$. The AF phase results from the interaction of two inversely polarized "ferromagnetic" square lattices.

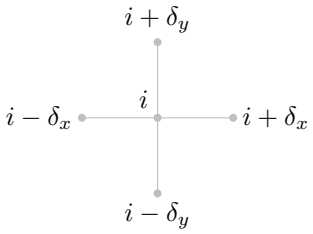

Figure 1.2 | Schematic representation of the four NNs of a given site i for a planar square lattice.

Note that, on a square lattice, we can perform the summation over NN just as

$$\sum_{\langle ij \rangle} \equiv \sum_{i \in \mathcal{S}_a} \left[\delta_{j=i+\delta_x} + \delta_{j=i-\delta_x} + \delta_{j=i+\delta_y} + \delta_{j=i-\delta_y} \right]$$

where notation of Fig. 1.1b has been used. The last term represents an effective attraction between neighboring electrons, of amplitude V. Such an interaction is believed [1] necessary to describe the insurgence of high-T_c superconductivity in cuprate SCs. [To be continued...]

1.2.1 Experimental insight on NN attraction

Todo:

- High T_c SC in cuprates;
- Experimental evidence of topological SC;
- Insertion of the non-local attraction;

1.3 Mean-Field theory description

This section is devoted to develop a rough mean field approximation of the Extended Hubbard model of Eq. (1.2). First part focuses on the non-local interaction V, expected to be source of superconductivity; the second part on the local interaction U, known to be source of Slater-like anti-ferromagnetism, as described in App. **??**.

1.3.1 Mean-field treatment of the non-local term

Consider the non-local term,

$$\hat{H}_V \equiv -V \sum_{\langle ij \rangle} \sum_{\sigma\sigma'} \hat{n}_{i\sigma} \hat{n}_{j\sigma'} \tag{1.3}$$

Since the relevant values for V are $\mathcal{O}(t)$, in this model $V \ll U$. Evidently the hamiltonian can be decomposed in various spin terms,

$$\begin{aligned} \hat{H}_V &= \sum_{\sigma\sigma'} \hat{H}_V^{\sigma\sigma'} \\ &= \underbrace{\hat{H}_V^{\uparrow\uparrow} + \hat{H}_V^{\downarrow\downarrow}}_{\text{Ferromagnetic}} + \underbrace{\hat{H}_V^{\uparrow\downarrow} + \hat{H}_V^{\downarrow\uparrow}}_{\text{Anti-ferromagnetic}} \end{aligned}$$

Evidently, to carry out a summation over nearest neighbors $\langle ij \rangle$ of a square lattice means precisely to sum over all links of the lattice. Then we can identify the generic AF term $\hat{H}_V^{\sigma\overline{\sigma}}$ as the one collecting the σ operators of sublattice $\mathcal{S}_a$ and $\overline{\sigma}$ operators of sublattice $\mathcal{S}_b$. At half-filling, as described in Sec. 1.1, the ground-state leading contribution will be the antiferromagnetic state, with the square lattice decomposed in two oppositely polarized square lattices with spacing increased by a factor $\sqrt{2}$. Then, it is to be expected that on this configuration the ferromagnetic contributions

are suppressed[1]. Anyways, the calculation will be carried out considering both terms. The AF non-local interactions can be written as a sum of terms over just one of the two sublattices $\mathcal{S}_a$ and $\mathcal{S}_b$, oppositely polarized in the AF configuration (see Fig. 1.1b)

$$\hat{H}_V^{(\mathrm{AF})} = \overbrace{\sum_{i\in\mathcal{S}_a} \hat{h}_V^{(i)}}^{\hat{H}_V^{\uparrow\downarrow}} + \overbrace{\sum_{i\in\mathcal{S}_b} \hat{h}_V^{(i)}}^{\hat{H}_V^{\downarrow\uparrow}} = \sum_{i\in\mathcal{S}} \hat{h}_V^{(i)} \qquad \hat{h}_V^{(i)} = -V \sum_{\ell=x,y} (\hat{n}_{i\uparrow}\hat{n}_{i+\delta_\ell\downarrow} + \hat{n}_{i\uparrow}\hat{n}_{i-\delta_\ell\downarrow})$$

Here the notation of Fig. 1.1b is used. The two-dimensional lattice is regular-square. For each site i in a given sublattice, the nearest neighbors sites are four – all in the other sublattice. The notation used is $i \pm \delta_x$, $i \pm \delta_y$ as in Fig. 1.2. Similarly, the Ferromagnetic hamiltonian decomposes as

$$\hat{H}_V^{(\mathrm{F})} = -V \sum_{i\in\mathcal{S}_a} \sum_{\ell=x,y} \sum_{\sigma} (\hat{n}_{i\sigma}\hat{n}_{i+\delta_\ell\sigma} + \hat{n}_{i\sigma}\hat{n}_{i-\delta_\ell\sigma})$$

Note here the summation only on one sublattice. As will be shown in Sec. 1.3.6, under MFT it makes sense to approximate

$$\hat{H}_V \simeq \hat{H}_V^{(\mathrm{AF})}$$

thus neglecting ferromagnetic contribution to Cooper instability. The non-local interaction contribution to energy, as a function of the $T = 0$ full hamiltonian ground-state[2] $|\Psi\rangle$, is given by

$$\begin{aligned} E_V[\Psi] &= \langle\Psi|\hat{H}_V|\Psi\rangle \\ &= -V \sum_{i\in\mathcal{S}} \sum_{\ell=x,y} \langle \hat{n}_{i\uparrow}\hat{n}_{i+\delta_\ell\downarrow} + \hat{n}_{i\uparrow}\hat{n}_{i-\delta_\ell\downarrow}\rangle \end{aligned}$$

Shorthand notation has been used: $\langle\Psi|\cdot|\Psi\rangle = \langle\cdot\rangle$. Consider one specific term, say, $\hat{n}_{i\uparrow}\hat{n}_{i+\delta_x\downarrow}$. Wick's Theorem states that, if the expectation value is performed onto a coherent state,

$$\begin{aligned} \langle \hat{n}_{i\uparrow}\hat{n}_{i+\delta_x\downarrow}\rangle &= \langle \hat{c}_{i\uparrow}^\dagger \hat{c}_{i+\delta_x\downarrow}^\dagger \hat{c}_{i+\delta_x\downarrow}\hat{c}_{i\uparrow}\rangle \\ &= \underbrace{\langle \hat{c}_{i\uparrow}^\dagger \hat{c}_{i+\delta_x\downarrow}^\dagger\rangle\langle \hat{c}_{i+\delta_x\downarrow}\hat{c}_{i\uparrow}\rangle}_{\text{Cooper}} - \underbrace{\langle \hat{c}_{i\uparrow}^\dagger \hat{c}_{i+\delta_x\downarrow}\rangle\langle \hat{c}_{i+\delta_x\downarrow}^\dagger \hat{c}_{i\uparrow}\rangle}_{\text{Fock}} + \underbrace{\langle \hat{c}_{i\uparrow}^\dagger \hat{c}_{i\uparrow}\rangle\langle \hat{c}_{i+\delta_x\downarrow}^\dagger \hat{c}_{i+\delta_x\downarrow}\rangle}_{\text{Hartree}} \end{aligned}$$

As a first approximation, the theorem is assumed to hold (which, in a BCS-like fashion, is equivalent to assuming for the ground-state to be a coherent state). The last two terms account for single-particle interactions with a background field; they are relevant in the Hartree-Fock scheme, being direct-exchange contributions to single particle energies. The first term accounts for non-local electrons pairing, mimicking the Cooper term of BCS theory. The core assumption, here, is that only one of the HF and Bogoliubov pairings survive. Appendix **??** shows a situation dominated by HF terms. Here, I assume the symmetry to be broken by a Cooper term. Energy then is cast to the form

$$E_V[\Psi] = -V \sum_{i\in\mathcal{S}} \sum_{\ell=x,y} \left[\langle \hat{c}_{i\uparrow}^\dagger \hat{c}_{i+\delta_\ell\downarrow}^\dagger\rangle\langle \hat{c}_{i+\delta_\ell\downarrow}\hat{c}_{i\uparrow}\rangle + \langle \hat{c}_{i\uparrow}^\dagger \hat{c}_{i-\delta_\ell\downarrow}^\dagger\rangle\langle \hat{c}_{i-\delta_\ell\downarrow}\hat{c}_{i\uparrow}\rangle \right]$$

The ground-state must realize the condition

$$\frac{\delta}{\delta\langle\Psi|} E[\Psi] = 0$$

[1] This is also due to superexchange stabilization: the triplet contribution to hamiltonian is suppressed, and this cancels out the ferromagnetic terms $\hat{H}_V^{\sigma\sigma}$ while privileging the singlet configuration of the anti-ferromagnetic terms $\hat{H}_V^{\sigma\bar{\sigma}}$.

[2] Extensions to finite temperatures is simple: minimization must be carried out on free energy, while expectation values must be taken in a thermodynamic fashion.

being $E[\Psi]$ the total energy (made up of the three terms of couplings t, U and V). [Expand derivation?] The functional derivative must be carried out in a variational fashion including a Lagrange multiplier, the latter accounting for state-norm conservation, as is done normally in deriving the Hartree-Fock approximation for the eigenenergies of the electron liquid [4, 5]. This approach leads to the conclusion that the (coherent) ground-state of the system must be an eigenstate of the mean-field effective hamiltonian:

$$\begin{aligned}\hat{H}^{(\mathrm{e})} = &- t \sum_{\langle ij \rangle} \sum_{\sigma} \hat{c}^{\dagger}_{i\sigma} \hat{c}_{j\sigma} + U \sum_{i \in \mathcal{S}} \hat{n}_{i\uparrow} \hat{n}_{i\downarrow} \\ &- V \sum_{i \in \mathcal{S}} \sum_{\ell = x,y} \sum_{\delta = \pm \delta_{\ell}} \left[\langle \hat{c}^{\dagger}_{i\uparrow} \hat{c}^{\dagger}_{i+\delta\downarrow} \rangle \hat{c}_{i+\delta\downarrow} \hat{c}_{i\uparrow} + \text{h.c.} \right]\end{aligned} \tag{1.4}$$

The pairing correlation function is defined across each bond as the pairing expectation

$$g_{ij\sigma} \equiv \langle \hat{c}^{\dagger}_{i\sigma} \hat{c}^{\dagger}_{j\overline{\sigma}} \rangle$$

The effective hamiltonian reads:

$$\hat{H}^{(\mathrm{e})} = -t \sum_{\langle ij \rangle} \sum_{\sigma} \hat{c}^{\dagger}_{i\sigma} \hat{c}_{j\sigma} + U \sum_{i \in \mathcal{S}} \hat{n}_{i\uparrow} \hat{n}_{i\downarrow} - V \sum_{\langle ij \rangle} \sum_{\sigma} \left[g_{ij\sigma} \hat{c}_{j\overline{\sigma}} \hat{c}_{i\sigma} + g^{*}_{ij\sigma} \hat{c}^{\dagger}_{i\sigma} \hat{c}^{\dagger}_{j\overline{\sigma}} \right] \tag{1.5}$$

As in standard BCS theory, this hamiltonian – being quadratic in the electronic operators – can be diagonalized via a Bogoliubov rotation. Superconducting pairing can arise both from the local U term and from the non-local V term. In next sections it is assumed the V term generates dominant superconductivity via its weak non-local pairing.

1.3.2 Mean-field treatment of the local term

The mean-field description of the local (on-site) U interaction is given in detail in App. **??**, along with a simple numerical analysis of the insurgence of antiferromagnetic ordering in a Hartree-Fock approximation scheme. Here the Cooper pairing is likewise assumed to dominate. Performing an analysis analogous to the one carried out in last section, we get the decoupling

$$U \sum_{i \in \mathcal{S}} \hat{n}_{i\uparrow} \hat{n}_{i\downarrow} \simeq \frac{U}{2} \sum_{i\sigma} \left[f_{i\sigma} \hat{c}_{i\overline{\sigma}} \hat{c}_{i\sigma} + f^{*}_{i\sigma} \hat{c}^{\dagger}_{i\sigma} \hat{c}^{\dagger}_{i\overline{\sigma}} \right]$$

being

$$f_{i\sigma} \equiv \langle \hat{c}^{\dagger}_{i\sigma} \hat{c}^{\dagger}_{i\overline{\sigma}} \rangle$$

Collect f and g in the unique function of two variables:

$$C_{\sigma}(i,j) = \begin{cases} f_{i\sigma} & \text{if} \quad i = j \\ g_{ij\sigma} & \text{if} \quad |i-j| = 1 \\ (\cdots) & \text{otherwise} \end{cases}$$

which expresses the generic correlator $\langle \hat{c}^{\dagger}_{i\sigma} \hat{c}^{\dagger}_{j\overline{\sigma}} \rangle$. The correlator for $|i-j| > 1$ is left unexpressed, and supposed to be subdominant. The decoupled hamiltonian, apart from pure energy shifts and suppressed terms, is given by

$$\begin{aligned}\hat{H}^{(\mathrm{e})} = &-t \sum_{\langle ij \rangle} \sum_{\sigma} \hat{c}^{\dagger}_{i\sigma} \hat{c}_{j\sigma} + \frac{U}{2} \sum_{i\sigma} \left[f_{i\sigma} \hat{c}_{i\overline{\sigma}} \hat{c}_{i\sigma} + f^{*}_{i\sigma} \hat{c}^{\dagger}_{i\sigma} \hat{c}^{\dagger}_{i\overline{\sigma}} \right] \\ &- V \sum_{\langle ij \rangle} \sum_{\sigma} \left[g_{ij\sigma} \hat{c}_{j\overline{\sigma}} \hat{c}_{i\sigma} + g^{*}_{ij\sigma} \hat{c}^{\dagger}_{i\sigma} \hat{c}^{\dagger}_{j\overline{\sigma}} \right]\end{aligned} \tag{1.6}$$

The last form of the full hamiltonian contains explicitly spin DoF. The dissertation that follows includes explicitly spin DoF.

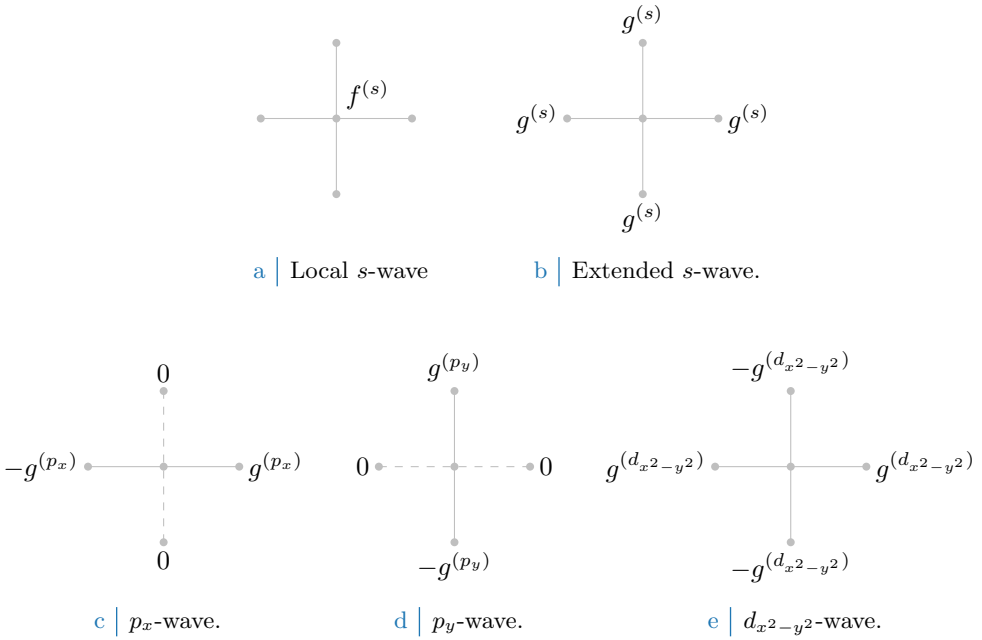

a | Local s-wave b | Extended s-wave.

c | p_x-wave. d | p_y-wave. e | $d_{x^2-y^2}$-wave.

Figure 1.3 | Different spatial structures of the correlation function under planar rotations. The figures show the first five local and NN contributions to the spatial structure of $C_\sigma(i,j)$. Each graph is a different contribution to the expansion of C_σ. Under each graph, each rim site contributes by a weight given by ± 1 or 0 times a constant dependent of the specific symmetry (f or g in figures), as specified in text.

Structure	Correlation function	Graph
s-wave	$f_i^{(s)} = f^{(s)}$	Fig. 1.3a
Extended s-wave	$g_{ij}^{(s)} = g^{(s)}\left(\delta_{j=i+\delta_x} + \delta_{j=i-\delta_x} + \delta_{j=i+\delta_y} + \delta_{j=i-\delta_y}\right)$	Fig. 1.3b
p_x-wave	$g_{ij}^{(p_x)} = g^{(p_x)}\left(\delta_{j=i+\delta_x} - \delta_{j=i-\delta_x}\right)$	Fig. 1.3c
p_y-wave	$g_{ij}^{(p_y)} = g^{(p_y)}\left(\delta_{j=i+\delta_y} - \delta_{j=i-\delta_y}\right)$	Fig. 1.3d
$d_{x^2-y^2}$-wave	$g_{ij}^{(d_{x^2-y^2})} = g^{(d_{x^2-y^2})}\left(\delta_{j=i+\delta_x} + \delta_{j=i-\delta_x} - \delta_{j=i+\delta_y} - \delta_{j=i-\delta_y}\right)$	Fig. 1.3e

Table 1.1 | First four spatial structures for the correlation function $C(i,j)$ (spin DoF is neglected). In the middle column, all spatial dependence is included in the δs, while $f^s, g^{(\ell)} \in \mathbb{C}$. The last column indicates the graph representation of each contribution given in Fig. 1.3.

1.3.3 Topological superconducting parameters over the square lattice

Consider Eq. (1.6), and for simplicity neglect the spin DoF in the last term.

The correlator g_{ij} is a function of position, specifically of its variables difference $r \equiv j - i$. Over the square lattice with NN interaction, the latter can assume four values: $\pm\delta_x$, $\pm\delta_y$. For a function of space defined over the four rim sites $i \pm \delta_\ell$ of Fig. 1.2, various symmetry structures can be defined under the planar rotations group SO(2). In other words, the function g_r can be decomposed in planar harmonics (which are simply the sine-cosine basis). Fig. 1.3 shows the first four spatial structures for the NN term. For each graph, the relative weight in the decomposition of g_r is given by a constant correlation $g^{(\ell)}$ times a sum of signs and zeros as indicated in the various subgraphs of Fig. 1.3. Tab. 1.1 reports said gap function contributions explicitly.

SC is established with a given symmetry – which means, symmetry breaking in the phase transition proceeds in a specific channel. Conventional BCS superconductivity arises from the only possible spatial structure of the local pairing, s-wave – here appearing as a local term (Fig. 1.3a) and extended on a non-local term (Fig. 1.3b). Cuprates exhibit a tendency towards $d_{x^2-y^2}$ SC, while other materials towards p-wave types – eventually with some chirality, as is the case for

$p_x \pm ip_y$ SCs.

In this BCS-like approach, a self-consistent equation for the gap function must be retrieved in order to further investigate the model and extract the conditions for the formation of a superconducting phase with a given pairing topology.

1.3.4 Reciprocal space transformation of hamiltonian

Let me take a step back and perform explicitly the Fourier-transform of the various terms of Eq. 1.2. MFT will be implemented later.

Kinetic term

The kinetic part is trivial to transform. Calculation is carried out in App. **??**. Let

$$\epsilon_{\mathbf{k}} \equiv -2t\left[\cos(k_x\delta_x) + \cos(k_y\delta_y)\right]$$

then we have

$$\begin{aligned}
-t\sum_{\langle ij\rangle}\sum_{\sigma}\hat{c}^{\dagger}_{i\sigma}\hat{c}_{j\sigma} &= \sum_{\mathbf{k}\sigma}\epsilon_{\mathbf{k}}\hat{c}^{\dagger}_{\mathbf{k}\sigma}\hat{c}_{\mathbf{k}\sigma} \\
&= \sum_{\mathbf{k}}\epsilon_{\mathbf{k}}\left[\hat{c}^{\dagger}_{\mathbf{k}\uparrow}\hat{c}_{\mathbf{k}\uparrow} + \hat{c}^{\dagger}_{\mathbf{k}\downarrow}\hat{c}_{\mathbf{k}\downarrow}\right] \\
&= \sum_{\mathbf{k}}\epsilon_{\mathbf{k}}\left[\hat{c}^{\dagger}_{\mathbf{k}\uparrow}\hat{c}_{\mathbf{k}\uparrow} - \hat{c}_{-\mathbf{k}\downarrow}\hat{c}^{\dagger}_{-\mathbf{k}\downarrow}\right]
\end{aligned}$$

In last passage I used fermionic anti-commutation rules and reversed the sign of the mute variable. This will become useful later.

Non-local interaction

Consider a generic bond, say, the one connecting sites j and $j \pm \delta_\ell$ (variable i is here referred to as the imaginary unit to avoid confusion). $\mathbf{x}_j$ is the 2D notation for the position of site j, while $\boldsymbol{\delta}_\ell$ is the 2D notation for the lattice spacing previously indicated as δ_ℓ. Fourier transform it according to the convention

$$\hat{c}_{j\sigma} = \frac{1}{\sqrt{L_xL_y}}\sum_{\mathbf{k}\in\mathrm{BZ}} e^{-i\mathbf{k}\cdot\mathbf{x}_j}\hat{c}_{\mathbf{k}\sigma}$$

Then:

$$\begin{aligned}
\hat{n}_{j\uparrow}\hat{n}_{j\pm\delta_\ell\downarrow} &= \hat{c}^{\dagger}_{j\uparrow}\hat{c}^{\dagger}_{j\pm\delta_\ell\downarrow}\hat{c}_{j\pm\delta_\ell\downarrow}\hat{c}_{j\uparrow} \\
&= \frac{1}{(L_xL_y)^2}\sum_{\nu=1}^{4}\sum_{\mathbf{k}_\nu\in\mathrm{BZ}} e^{i[(\mathbf{k}_1+\mathbf{k}_2)-(\mathbf{k}_3+\mathbf{k}_4)]\cdot\mathbf{x}_j}e^{\pm i(\mathbf{k}_2-\mathbf{k}_3)\cdot\boldsymbol{\delta}_\ell}\hat{c}^{\dagger}_{\mathbf{k}_1\uparrow}\hat{c}^{\dagger}_{\mathbf{k}_2\downarrow}\hat{c}_{\mathbf{k}_3\downarrow}\hat{c}_{\mathbf{k}_4\uparrow}
\end{aligned}$$

It follows,

$$\begin{aligned}
\hat{h}^{(j)}_V &= -\frac{V}{(L_xL_y)^2}\sum_{\ell=x,y}\sum_{\nu=1}^{4}\sum_{\mathbf{k}_\nu\in\mathrm{BZ}} e^{i[(\mathbf{k}_1+\mathbf{k}_2)-(\mathbf{k}_3+\mathbf{k}_4)]\cdot\mathbf{x}_j} \\
&\qquad\qquad \times\left(e^{i(\mathbf{k}_2-\mathbf{k}_3)\cdot\boldsymbol{\delta}_\ell} + e^{-i(\mathbf{k}_2-\mathbf{k}_3)\cdot\boldsymbol{\delta}_\ell}\right)\hat{c}^{\dagger}_{\mathbf{k}_1\uparrow}\hat{c}^{\dagger}_{\mathbf{k}_2\downarrow}\hat{c}_{\mathbf{k}_3\downarrow}\hat{c}_{\mathbf{k}_4\uparrow} \\
&= -\frac{2V}{(L_xL_y)^2}\sum_{\ell=x,y}\sum_{\nu=1}^{4}\sum_{\mathbf{k}_\nu\in\mathrm{BZ}} e^{i[(\mathbf{k}_1+\mathbf{k}_2)-(\mathbf{k}_3+\mathbf{k}_4)]\cdot\mathbf{x}_j}\cos\left[(\mathbf{k}_2-\mathbf{k}_3)\cdot\boldsymbol{\delta}_\ell\right]\hat{c}^{\dagger}_{\mathbf{k}_1\uparrow}\hat{c}^{\dagger}_{\mathbf{k}_2\downarrow}\hat{c}_{\mathbf{k}_3\downarrow}\hat{c}_{\mathbf{k}_4\uparrow}
\end{aligned}$$

The full non-local interaction is given by summing over all sites of $\mathcal{S}$. This gives back momentum conservation,

$$\frac{1}{L_xL_y}\sum_{j\in\mathcal{S}} e^{i[(\mathbf{k}_1+\mathbf{k}_2)-(\mathbf{k}_3+\mathbf{k}_4)]\cdot\mathbf{x}_j} = \delta_{\mathbf{k}_1+\mathbf{k}_2=\mathbf{k}_3+\mathbf{k}_4}$$

Let $\mathbf{k}_1 + \mathbf{k}_2 = \mathbf{k}_3 + \mathbf{k}_4 = \mathbf{K}$, and define $\mathbf{k}$, $\mathbf{k}'$ such that

$$\mathbf{k}_1 \equiv \mathbf{K} + \mathbf{k} \qquad \mathbf{k}_2 \equiv \mathbf{K} - \mathbf{k} \qquad \mathbf{k}_3 \equiv \mathbf{K} - \mathbf{k}' \qquad \mathbf{k}_4 \equiv \mathbf{K} + \mathbf{k}' \qquad \delta\mathbf{k} \equiv \mathbf{k} - \mathbf{k}'$$

Sums over these variables must be intended as over the Brillouin Zone (BZ). Then, finally

$$\begin{aligned}
\hat{H}_V &\simeq \sum_{j\in\mathcal{S}} \hat{h}_V^{(j)} \\
&= -\frac{2V}{L_x L_y} \sum_{\ell=x,y} \sum_{\mathbf{K},\mathbf{k},\mathbf{k}'} \cos\left(\delta\mathbf{k}\cdot\boldsymbol{\delta}_\ell\right) \hat{c}^\dagger_{\mathbf{K}+\mathbf{k}\uparrow} \hat{c}^\dagger_{\mathbf{K}-\mathbf{k}\downarrow} \hat{c}_{\mathbf{K}-\mathbf{k}'\downarrow} \hat{c}_{\mathbf{K}+\mathbf{k}'\uparrow} \\
&= -\frac{2V}{L_x L_y} \sum_{\ell=x,y} \sum_{\mathbf{K},\mathbf{k},\mathbf{k}'} \left[\cos\left(\delta k_x \delta_x\right) + \cos\left(\delta k_y \delta_y\right)\right] \hat{c}^\dagger_{\mathbf{K}+\mathbf{k}\uparrow} \hat{c}^\dagger_{\mathbf{K}-\mathbf{k}\downarrow} \hat{c}_{\mathbf{K}-\mathbf{k}'\downarrow} \hat{c}_{\mathbf{K}+\mathbf{k}'\uparrow}
\end{aligned}$$

Eventually, in the second passage the prefactor 2 can be absorbed by reintroducing the spin DoF[3]. Taking in the mean-field approximation (with Cooper pair symmetry breaking), we get

$$\hat{c}^\dagger_{\mathbf{K}+\mathbf{k}\uparrow} \hat{c}^\dagger_{\mathbf{K}-\mathbf{k}\downarrow} \hat{c}_{\mathbf{K}-\mathbf{k}'\downarrow} \hat{c}_{\mathbf{K}+\mathbf{k}'\uparrow} \simeq \langle \hat{c}^\dagger_{\mathbf{K}+\mathbf{k}\uparrow} \hat{c}^\dagger_{\mathbf{K}-\mathbf{k}\downarrow} \rangle \hat{c}_{\mathbf{K}-\mathbf{k}'\downarrow} \hat{c}_{\mathbf{K}+\mathbf{k}'\uparrow} + \hat{c}^\dagger_{\mathbf{K}+\mathbf{k}\uparrow} \hat{c}^\dagger_{\mathbf{K}-\mathbf{k}\downarrow} \langle \hat{c}_{\mathbf{K}-\mathbf{k}'\downarrow} \hat{c}_{\mathbf{K}+\mathbf{k}'\uparrow} \rangle + \cdots$$

Take e.g. $\langle \hat{c}^\dagger_{\mathbf{K}+\mathbf{k}\uparrow} \hat{c}^\dagger_{\mathbf{K}-\mathbf{k}\downarrow} \rangle$: the only non-zero contribution can come from the $\mathbf{K} = \mathbf{0}$ term, as will be discussed self-consistently in Sec. 1.3.6. Then finally:

$$\hat{H}_V \simeq -\frac{2V}{L_x L_y} \sum_{\mathbf{k},\mathbf{k}'} \left[\cos\left(\delta k_x \delta_x\right) + \cos\left(\delta k_y \delta_y\right)\right] \left[\langle \hat{c}^\dagger_{\mathbf{k}\uparrow} \hat{c}^\dagger_{-\mathbf{k}\downarrow} \rangle \hat{\phi}_{\mathbf{k}'} + \langle \hat{c}_{-\mathbf{k}\downarrow} \hat{c}_{\mathbf{k}\uparrow} \rangle \hat{\phi}^\dagger_{\mathbf{k}'} \right]$$

having I defined the pairing operator

$$\hat{\phi}_{\mathbf{k}} \equiv \hat{c}_{-\mathbf{k}\downarrow} \hat{c}_{\mathbf{k}\uparrow}$$

Defining appropriately the non-local gap function,

$$\mathcal{V}_{\mathbf{k}} \equiv \frac{2V}{L_x L_y} \sum_{\mathbf{k}'} \left[\cos\left((k_x - k'_x)\delta_x\right) + \cos\left((k_y - k'_y)\delta_y\right)\right] \langle \hat{c}^\dagger_{\mathbf{k}'\uparrow} \hat{c}^\dagger_{-\mathbf{k}'\downarrow} \rangle \tag{1.7}$$

one gets immediately

$$\hat{H}_V \simeq -\sum_{\mathbf{k}} \left[\mathcal{V}_{\mathbf{k}} \hat{\phi}_{\mathbf{k}} + \mathcal{V}^*_{\mathbf{k}} \hat{\phi}^\dagger_{\mathbf{k}} \right] \tag{1.8}$$

The non-local interaction has been reduced, by MFT, to particle-background interaction for the ϕ-fermions.

Local interaction

A very similar argument can be carried out for the local U term. Without delving in too many details, the local gap $\mathcal{U}_{\mathbf{k}}$ is given by

$$\mathcal{U}_{\mathbf{k}} \equiv \frac{U}{2L_x L_y} \sum_{\mathbf{k}'} \langle \hat{c}^\dagger_{\mathbf{k}'\uparrow} \hat{c}^\dagger_{-\mathbf{k}'\downarrow} \rangle \tag{1.9}$$

evidently independent of $\mathbf{k}$, correctly. The local part of the hamiltonian then gets

$$\hat{H}_U = \sum_{\mathbf{k}} \left[\mathcal{U}_{\mathbf{k}} \hat{\phi}_{\mathbf{k}} + \mathcal{U}^*_{\mathbf{k}} \hat{\phi}^\dagger_{\mathbf{k}} \right] \tag{1.10}$$

The total gap is thus given by the simple difference of non-local and local parts,

$$\Delta_{\mathbf{k}} \equiv \mathcal{V}_{\mathbf{k}} - \mathcal{U}_{\mathbf{k}}$$

Within this structure, we are finally able to move to Nambu formalism.

[3] Justification can be given in two ways: either commutating appropriately the $\hat{c}$ operators, or by carrying out the previous space sums independently over the two sublattices.

1.3.5 Nambu formalism and Bogoliubov transform

Define the Nambu spinor[4] as in BCS

$$\hat{\Psi}_{\mathbf{k}} \equiv \begin{bmatrix} \hat{c}_{\mathbf{k}\uparrow} \\ \hat{c}^{\dagger}_{-\mathbf{k}\downarrow} \end{bmatrix}$$

Evidently,

$$\phi_{\mathbf{k}} = \hat{\Psi}^{\dagger}_{\mathbf{k}} \begin{bmatrix} 0 & 1 \\ 0 & 0 \end{bmatrix} \hat{\Psi}_{\mathbf{k}} \qquad \phi^{\dagger}_{\mathbf{k}} = \hat{\Psi}^{\dagger}_{\mathbf{k}} \begin{bmatrix} 0 & 0 \\ 1 & 0 \end{bmatrix} \hat{\Psi}_{\mathbf{k}} \tag{1.11}$$

The full hamiltonian is then given by:

$$\hat{H} = \sum_{\mathbf{k}} \hat{\Psi}_{\mathbf{k}} h_{\mathbf{k}} \hat{\Psi}_{\mathbf{k}} \qquad h_{\mathbf{k}} \equiv \begin{bmatrix} \epsilon_{\mathbf{k}} & -\Delta^{*}_{\mathbf{k}} \\ -\Delta_{\mathbf{k}} & -\epsilon_{\mathbf{k}} \end{bmatrix} \tag{1.12}$$

Let τ^{α} for $\alpha = x, y, z$ be the Pauli matrices. Define:

$$\hat{s}^{\alpha}_{\mathbf{k}} \equiv \hat{\Psi}^{\dagger}_{\mathbf{k}} \tau^{\alpha} \hat{\Psi}_{\mathbf{k}} \quad \text{for} \quad \alpha = x, y, z$$

As can be shown easily, these operators realize spin-1/2 algebra. $\hat{H}$ represents an ensemble of $L_x L_y$ independent spins subject to pseudo-magnetic fields. Note that, differently form App. **??** where the chemical potential is inserted later (because in Nambu formalism it accounts for a diagonal term) here the chemical potential is part of the z component of the pseudo-magnetic field, since

$$\begin{aligned} \hat{n}_{\mathbf{k}\uparrow} + \hat{n}_{-\mathbf{k}\downarrow} &= \hat{c}^{\dagger}_{\mathbf{k}\uparrow} \hat{c}_{\mathbf{k}\uparrow} + \hat{c}^{\dagger}_{-\mathbf{k}\downarrow} \hat{c}_{-\mathbf{k}\downarrow} \\ &= \hat{c}^{\dagger}_{\mathbf{k}\uparrow} \hat{c}_{\mathbf{k}\uparrow} - \hat{c}_{-\mathbf{k}\downarrow} \hat{c}^{\dagger}_{-\mathbf{k}\downarrow} + \mathbb{I} \\ &= \hat{\Psi}^{\dagger}_{\mathbf{k}} \tau^{z} \hat{\Psi}_{\mathbf{k}} + \mathbb{I} \end{aligned} \tag{1.13}$$

and then it follows

$$\begin{aligned} -\mu \hat{N} &= -\mu \sum_{\mathbf{k} \in \mathrm{BZ}} [\hat{n}_{\mathbf{k}\uparrow} + \hat{n}_{-\mathbf{k}\downarrow}] \\ &= -\mu \sum_{\mathbf{k} \in \mathrm{BZ}} \hat{\Psi}^{\dagger}_{\mathbf{k}} \tau^{z} \hat{\Psi}_{\mathbf{k}} - \mu L_x L_y \end{aligned}$$

Then, adding a term $-\mu \hat{N}$ to $\hat{H}$, apart from an irrelevant total energy increase, changes the pseudo-field whose explicit form becomes

$$\mathbf{b}_{\mathbf{k}} \equiv \begin{bmatrix} -\operatorname{Re}\{\Delta_{\mathbf{k}}\} \\ -\operatorname{Im}\{\Delta_{\mathbf{k}}\} \\ \epsilon_{\mathbf{k}} - \mu \end{bmatrix} \tag{1.14}$$

This hamiltonian behaves as an ensemble of spins in local magnetic fields precisely as in Eq. (**??**),

$$\hat{H} - \mu \hat{N} = \sum_{\mathbf{k} \in \mathrm{BZ}} \mathbf{b}_{\mathbf{k}} \cdot \hat{\mathbf{s}}_{\mathbf{k}} \quad \text{where} \quad \hat{\mathbf{s}}_{\mathbf{k}\sigma} = \begin{bmatrix} \hat{s}^{x}_{\mathbf{k}} \\ \hat{s}^{y}_{\mathbf{k}} \\ \hat{s}^{z}_{\mathbf{k}} \end{bmatrix} \tag{1.15}$$

Proceed as in App. **??** and diagonalize via a rotation,

$$d_{\mathbf{k}} \equiv \begin{bmatrix} -E_{\mathbf{k}} & \\ & E_{\mathbf{k}} \end{bmatrix} \quad \text{being} \quad E_{\mathbf{k}} \equiv \sqrt{(\epsilon_{\mathbf{k}} - \mu)^2 + |\Delta_{\mathbf{k}}|^2}$$

An HF algorithm requires iterative update of the order parameter. The general strategy here is to try different symmetry breaking structures via a set of self-consistency equations. From Eqns. (1.7), (1.9) we have formulas to calculate $\Delta_{\mathbf{k}}$ and $\mathcal{U}_{\mathbf{k}}$. Given the pseudoangles

$$\tan(2\theta_{\mathbf{k}}) \equiv \frac{|\Delta_{\mathbf{k}}|}{\epsilon_{\mathbf{k}}} \qquad \tan(2\varphi_{\mathbf{k}}) \equiv \frac{\operatorname{Im}\{\Delta_{\mathbf{k}}\}}{\operatorname{Re}\{\Delta_{\mathbf{k}}\}}$$

[4] Notice that the spinor is here differently defined with respect to App. **??**, where because of the HF prevalence in mean-field decoupling the spinor components were homogeneously fermions creations or destructions.

the general diagonalizer will be an orthogonal rotation matrix

$$\begin{aligned} W_{\mathbf{k}} &= e^{i\left(\theta_{\mathbf{k}}-\frac{\pi}{2}\right)\tau^y} e^{i\varphi_{\mathbf{k}}\tau^z} \\ &= \begin{bmatrix} -\sin\theta_{\mathbf{k}} & -\cos\theta_{\mathbf{k}} \\ \cos\theta_{\mathbf{k}} & -\sin\theta_{\mathbf{k}} \end{bmatrix} \begin{bmatrix} e^{i\varphi_{\mathbf{k}}} & \\ & e^{-i\varphi_{\mathbf{k}}} \end{bmatrix} \\ &= \begin{bmatrix} -\sin\theta_{\mathbf{k}} e^{i\varphi_{\mathbf{k}}} & -\cos\theta_{\mathbf{k}} e^{-i\varphi_{\mathbf{k}}} \\ \cos\theta_{\mathbf{k}} e^{i\varphi_{\mathbf{k}}} & -\sin\theta_{\mathbf{k}} e^{-i\varphi_{\mathbf{k}}} \end{bmatrix} \end{aligned} \tag{1.16}$$

given by a rotation of angle $\varphi_{\mathbf{k}}$ around the z axis, to align the x axis with the field projection onto the xy plane, followed by a rotation around the y axis to anti-align with the pseudo-field. The diagonalization operators are given by

$$\hat{\Phi}_{\mathbf{k}} \equiv W_{\mathbf{k}} \hat{\Psi}_{\mathbf{k}}$$

then, using Eq. (**??**),

$$\left\langle [\hat{\Psi}^\dagger_{\mathbf{k}}]_i [\hat{\Psi}_{\mathbf{k}}]_j \right\rangle = [W_{\mathbf{k}}]_{1i} [W^\dagger_{\mathbf{k}}]_{j1} f\left(-E_{\mathbf{k}}; \beta, 0\right) + [W_{\mathbf{k}}]_{2i} [W^\dagger_{\mathbf{k}}]_{j2} f\left(E_{\mathbf{k}}; \beta, 0\right)$$

where in the Fermi-Dirac function chemical potential was set to zero, because it already was included in the diagonalized hamiltonian. Recalling Eq. (1.11), it follows

$$\langle \phi_{\mathbf{k}} \rangle = [W_{\mathbf{k}}]_{12} [W^\dagger_{\mathbf{k}}]_{11} f\left(-E_{\mathbf{k}}; \beta, 0\right) + [W_{\mathbf{k}}]_{22} [W^\dagger_{\mathbf{k}}]_{12} f\left(E_{\mathbf{k}}; \beta, 0\right) \tag{1.17}$$

$$\langle \phi^\dagger_{\mathbf{k}} \rangle = [W_{\mathbf{k}}]_{11} [W^\dagger_{\mathbf{k}}]_{21} f\left(-E_{\mathbf{k}}; \beta, 0\right) + [W_{\mathbf{k}}]_{21} [W^\dagger_{\mathbf{k}}]_{22} f\left(E_{\mathbf{k}}; \beta, 0\right) \tag{1.18}$$

These equations give us the formulas to compute the order parameters in the HF approach, directly by their definitions of Eqns. (1.7), (1.9). At each point in k-space (k_x, k_y), the matrix $h_{\mathbf{k}}$ is diagonalized and the diagonalizer entries $[W_{\mathbf{k}}]_{ij}$ are combined in this fashion to recover the pairing expectation. The z component of the spin operators is related to density: using Eq. (**??**),

$$\langle \hat{\Psi}^\dagger_{\mathbf{k}} \tau^z \hat{\Psi}_{\mathbf{k}} \rangle = \left\langle [\hat{\Psi}^\dagger_{\mathbf{k}}]_1 [\hat{\Psi}_{\mathbf{k}}]_1 \right\rangle - \left\langle [\hat{\Psi}^\dagger_{\mathbf{k}}]_2 [\hat{\Psi}_{\mathbf{k}}]_2 \right\rangle$$

we get, from Eq. (1.13),

$$\begin{aligned} \langle \hat{n}_{\mathbf{k}\uparrow} \rangle + \langle \hat{n}_{-\mathbf{k}\downarrow} \rangle &= 1 + \langle \hat{\Psi}^\dagger_{\mathbf{k}} \tau^z \hat{\Psi}_{\mathbf{k}} \rangle \\ &= 1 + \left(|[W_{\mathbf{k}}]_{11}|^2 - |[W_{\mathbf{k}}]_{12}|^2 \right) f\left(-E_{\mathbf{k}}; \beta, 0\right) \\ &\quad + \left(|[W_{\mathbf{k}}]_{21}|^2 - |[W_{\mathbf{k}}]_{22}|^2 \right) f\left(E_{\mathbf{k}}; \beta, 0\right) \\ &= 1 - \cos\left(2\theta_{\mathbf{k}}\right) \tanh\left(\frac{\beta E_{\mathbf{k}}}{2}\right) \end{aligned} \tag{1.19}$$

the last passage obtained by computing the matrix element from the explicit form of $W_{\mathbf{k}}$ of Eq. (1.16) and by the simple relation

$$\begin{aligned} \frac{1}{e^{-x}+1} - \frac{1}{e^{x}+1} &= \frac{e^x - 1}{e^x + 1} \\ &= \tanh\left(\frac{x}{2}\right) \end{aligned}$$

The expectation value for the density is needed in order to extract the optimal chemical potential μ for the target density we aim to simulate at the given parametrization.

1.3.6 A short comment on self-consistency

The Bogoliubov fermions in spinor representation satisfy obviously $\hat{\Psi}_{\mathbf{k}} = W^\dagger_{\mathbf{k}} \hat{\Phi}_{\mathbf{k}}$. Consider e.g.

$$\langle \hat{c}^\dagger_{\mathbf{k}\sigma} \hat{c}^\dagger_{-\mathbf{k}\sigma} \rangle$$

which is a spin-symmetric anomalous Cooper pair. For simplicity, take $\sigma =\uparrow$. Expand:

$$\begin{aligned}\langle \hat{c}^\dagger_{\mathbf{k}\uparrow}\hat{c}^\dagger_{-\mathbf{k}\uparrow}\rangle &= \left\langle [\hat{\Psi}^\dagger_{\mathbf{k}}]_1[\hat{\Psi}^\dagger_{-\mathbf{k}}]_1 \right\rangle \\ &= \left\langle [W_{\mathbf{k}}\hat{\Phi}^\dagger_{\mathbf{k}}]_1[W_{-\mathbf{k}}\hat{\Phi}^\dagger_{-\mathbf{k}}]_1 \right\rangle\end{aligned}$$

This expectation value is taken over the ground-state, the latter being the vacuum of Φ fermions. Evidently the above expectation cannot assume non-zero values. Obviously the same holds for $\sigma =\downarrow$, and this argument explains why the Ferromagnetic terms of the hamiltonian decomposition do not contribute to Cooper instability. An identical argument, with the exchange

$$(\sigma,\sigma)\to(\uparrow,\downarrow) \quad \text{and} \quad (\mathbf{k},-\mathbf{k})\to(\mathbf{K}+\mathbf{k},\mathbf{K}-\mathbf{k}) \quad \text{with} \quad \mathbf{K}\neq\mathbf{0}$$

justifies why in Sec. 1.3.5 the only relevant contribution was given by $\mathbf{K}=\mathbf{0}$.

1.3.7 Non-local gap structures

Let's have a closer look to Eq. (1.7): performing explicitly

$$\begin{aligned}\langle \hat{c}^\dagger_{\mathbf{k}\sigma}\hat{c}^\dagger_{-\mathbf{k}\bar{\sigma}}\rangle &= \frac{1}{L_xL_y}\sum_{ij} e^{i\mathbf{k}\cdot(\mathbf{x}_i-\mathbf{x}_j)}C_\sigma(i,j) \\ &= \frac{1}{L_xL_y}\sum_{i\in\mathcal{S}} f_{i\sigma} + \frac{1}{L_xL_y}\sum_{\langle ij\rangle} e^{i\mathbf{k}\cdot(\mathbf{x}_i-\mathbf{x}_j)}g_{ij\sigma} + (\text{subdominant})\end{aligned}$$

Contributions to $C_\sigma(i,j)$ from $|i-j|>1$ are assumed to be subdominant and then neglected. The above equation needs to be equipped with some structure for $f_{i\sigma}$ and $g_{ij\sigma}$. The main idea is to try different channels of symmetry breaking starting from the gap function structures of Tab. 1.1 and follow the general HF procedure sketched in detail in App. **??**. An iterative algorithm will be carried out to estimate, rather roughly, the creation of an instability towards a precise topological superconducting pairing. Before doing so, notice that $g_{ij\sigma}$ is actually a function of $r=j-i$ (in vectorial notation: $\boldsymbol{\delta}_\ell=\mathbf{x}_j-\mathbf{x}_i$, with $\ell\in\{x,y\}$) in the symmetries we are considering, listed in Tab. 1.1. Thus

$$\langle \hat{c}^\dagger_{\mathbf{k}\sigma}\hat{c}^\dagger_{-\mathbf{k}\bar{\sigma}}\rangle = f^{(s)} + \sum_{\ell=x,y}\left[e^{i\mathbf{k}\cdot\boldsymbol{\delta}_\ell}g_{\boldsymbol{\delta}_\ell\sigma} + e^{-i\mathbf{k}\cdot\boldsymbol{\delta}_\ell}g_{-\boldsymbol{\delta}_\ell\sigma}\right] \tag{1.20}$$

Here, the simple uniform Ansatz for the f term has been included. By using the simple structures of Fig. 1.3 for the g function, this expression simplifies a lot. Moreover, considering the terms of Eq. (1.7),

$$\begin{aligned}\cos(\delta k_x\delta_x)+\cos(\delta k_y\delta_y) = \cos(k_x\delta_x)\cos(k'_x\delta_x)+\sin(k_x\delta_x)\sin(k'_x\delta_x) \\ +\cos(k_y\delta_y)\cos\left(k'_y\delta_y\right)+\sin(k_y\delta_y)\sin\left(k'_y\delta_y\right)\end{aligned}$$

For the sake of readability, the notations

$$c_\ell\equiv\cos(k_\ell\delta_\ell) \qquad s_\ell\equiv\sin(k_\ell\delta_\ell) \qquad c'_\ell\equiv\cos(k'_\ell\delta_\ell) \qquad s'_\ell\equiv\sin(k'_\ell\delta_\ell)$$

are used. Group the four terms above,

$$\underbrace{\left(c_xc'_x+c_yc'_y\right)}_{\text{Symmetric}}+\underbrace{\left(s_xs'_x+s_ys'_y\right)}_{\text{Anti-symmetric}} \tag{1.21}$$

Since sums on $\mathbf{k}$, $\mathbf{k}'$ are carried out, based on the specific $g_{\mathbf{k}}$ symmetry structures one can eliminate one of the two contributions. Take e.g. the p_x gap structure of Fig. 1.3c, listed in Tab. 1.1: since it exhibits spatial anti-symmetry on the x direction and (trivial) symmetry on the y direction, of the above terms only the x anti-symmetric part will contribute – which is, $s_xs'_x$. This property becomes useful in the next paragraphs, where detailed derivations on the spatial structures of the gap function are carried out. Results are listed in Tat. 1.2.

Structure	Gap function	Graph
s-wave	$\mathcal{U}_{\mathbf{k}} = \mathcal{U}^{(s)}$	Fig. 1.3a
Extended s-wave	$\mathcal{V}^{(s)}_{\mathbf{k}} = \mathcal{V}^{(s)}\left[\cos(k_x) + \cos(k_y)\right]$	Fig. 1.3b
p_x-wave	$\mathcal{V}^{(p_x)}_{\mathbf{k}} = i\mathcal{V}^{(p_x)}\sin(k_x)$	Fig. 1.3c
p_y-wave	$\mathcal{V}^{(p_y)}_{\mathbf{k}} = i\mathcal{V}^{(p_y)}\sin(k_y)$	Fig. 1.3d
$d_{x^2-y^2}$-wave	$\mathcal{V}^{(d)}_{\mathbf{k}} = \mathcal{V}^{(d)}\left[\cos(k_x) - \cos(k_y)\right]$	Fig. 1.3e

Table 1.2 | Gap structures for the four spatial symmetries of Fig. 1.3.

Extended s-wave gap structure

The standard s-wave structure of the gap function in BCS theory is given by the local interaction of Fig. 1.3a. Consider also its NN extension of Fig. 1.3b, we will refer to also as "s^*-wave". It is completely symmetric under rotations and inversions, thus it couples trivially to the symmetric part of the decoupling (1.21). Eq. (1.20) becomes:

$$\langle \hat{c}^\dagger_{\mathbf{k}\sigma} \hat{c}^\dagger_{-\mathbf{k}\bar{\sigma}} \rangle = f^{(s)} + 2g^{(s)}(c_x + c_y)$$

Performing the computation of Eq. (1.7) within this approximation, we get:

$$\mathcal{V}^{(s)}_{\mathbf{k}} = \frac{2V}{L_x L_y} \sum_{\mathbf{k}'} (c_x c'_x + c_y c'_y) \left[f^{(s)} + 2g^{(s)}(c'_x + c'_y) \right]$$
$$\mathcal{U}^{(s)}_{\mathbf{k}} = \frac{U}{2L_x L_y} \sum_{\mathbf{k}'} \left[f^{(s)} + 2g^{(s)}(c'_x + c'_y) \right]$$

Evidently $\sum_{\mathbf{k}'} c'_\ell = 0$. Then in the expression for $\mathcal{V}^{(s)}_{\mathbf{k}}$ the f part is suppressed, and likewise is the g part in the $\mathcal{U}^{(s)}_{\mathbf{k}}$ equation. Take a continuum approximation,

$$\frac{1}{L_x L_y} \sum_{\mathbf{k}'} c_\ell (c'_\ell)^2 \simeq c_\ell \int_{-\pi}^{\pi} \frac{ds}{2\pi} \cos^2 s = \frac{c_\ell}{2}$$
$$\frac{1}{L_x L_y} \sum_{\mathbf{k}'} c_\ell (c'_\ell c'_{\bar{\ell}}) \simeq c_\ell \left[\int_{-\pi}^{\pi} \frac{ds}{2\pi} \cos s \right]^2 = 0$$

It follows:

$$\mathcal{V}^{(s)}_{\mathbf{k}} = \mathcal{V}^{(s)}(c_x + c_y) \qquad \mathcal{U}^{(s)}_{\mathbf{k}} = \mathcal{U}^{(s)} \tag{1.22}$$

where $\mathcal{V}^{(s)} \equiv V \times 2g^{(s)}$ and $\mathcal{U}^{(s)} \equiv U \times f^{(s)}/2$. The quantity $\mathcal{V}^{(s)}$ is the order parameter in our HF scheme.

p_ℓ-wave gap structure

Take $\ell \in \{x, y\}$ and consider the p_ℓ-wave correlation in Tab. 1.1. Due to its anti-symmetry, it couples only to the antisymmetric part of (1.21). From Eq. (1.20),

$$\langle \hat{c}^\dagger_{\mathbf{k}\sigma} \hat{c}^\dagger_{-\mathbf{k}\bar{\sigma}} \rangle = 2ig^{(p_\ell)} s_\ell$$

and then from Eq. (1.7)

$$\mathcal{V}^{(p_\ell)}_{\mathbf{k}} = 2ig^{(p_\ell)} \frac{2V}{L_x L_y} \sum_{\mathbf{k}'} (s_x s'_x + s_y s'_y) s'_\ell$$

Using identical reasoning as above,

$$\mathcal{V}^{(p_\ell)}_{\mathbf{k}} = i\mathcal{V}^{(p_\ell)} s_\ell$$

where $\mathcal{V}^{(p_\ell)} \equiv V \times 2g^{(p_\ell)}$.

d-wave gap structure

Consider a $d_{x^2-y^2}$-wave structured gap function as in Fig. 1.3e The discourse here is perfectly analogous to Sec. 1.3.7, with the only difference

$$c_x + c_y \quad \rightarrow \quad c_x - c_y$$

Then the d-wave gap has the structure

$$\mathcal{V}_{\mathbf{k}}^{(d)} = \mathcal{V}^{(d)}(c_x - c_y) \tag{1.23}$$

where $\mathcal{V}^{(d)} \equiv V \times 2g^{(d)}$. Subscript $x^2 - y^2$ has been omitted for reasons of clarity.

1.3.8 Algorithmic reconstruction of the gap topology

[This section was included to account for a multi-symmetry gap function search algorithm.]

Proceeding as in Sec. 1.3.5, at each step we are able to recover $\mathcal{U}_{\mathbf{k}}$ and $\mathcal{V}_{\mathbf{k}}$. Indeed, simply diagonalizing $h_{\mathbf{k}}$ and using Eq. (1.18) we recover $\langle\hat{\phi}_{\mathbf{k}}\rangle$; then, by reconstruction, we use Eqns. (1.7) and (1.9) to get $\mathcal{U}_{\mathbf{k}}$ and $\mathcal{V}_{\mathbf{k}}$. Last step is to distinguish different topologies. From Tab. 1.2, we see

$$\Gamma_{\mathbf{k}} = \Gamma^{(\ell)} f_\ell(\mathbf{k}) \qquad \Gamma = \Sigma, \Delta \qquad \ell = s, p_x, p_y, d_{x^2-y^2}$$

being $f_\ell(\mathbf{k}) \in \mathbb{C}$ the structure factor at topology ℓ. Evidently,

$$\frac{1}{L_x L_y} \sum_{\mathbf{k}\in \mathrm{BZ}} \Gamma_{\mathbf{k}} f^*_{\ell'}(\mathbf{k}) \simeq \int_{\mathrm{BZ}} \frac{d\mathbf{k}}{(2\pi)^2} \Gamma_{\mathbf{k}} f^*_{\ell'}(\mathbf{k}) = \Gamma^{(\ell)} \delta_{\ell\ell'}$$

thus, in order to recover Γ^ℓ for a generic ℓ, using wave decomposition orthogonality rules it suffices to multiply the measured $\Gamma_{\mathbf{k}}$ by the appropriate structure factor, sum over the BZ and finally divide by the lattice volume.

Bibliography

[1] Zhangkai Cao et al. *p-wave superconductivity induced by nearest-neighbor attraction in the square-lattice extended Hubbard model*. en. arXiv:2408.01113 [cond-mat]. Jan. 2025. DOI: 10.48550/arXiv.2408.01113. URL: http://arxiv.org/abs/2408.01113 (visited on 03/15/2025).

[2] Piers Coleman. *Introduction to Many-Body Physics*. Cambridge University Press, 2015.

[3] Michele Fabrizio. *A Course in Quantum Many-Body Theory*. Springer, 2022.

[4] Gabriele Giuliani and Giovanni Vignale. *Quantum Theory of the Electron Liquid*. Cambridge University Press, 2005.

[5] Giuseppe Grosso and Giuseppe Pastori Parravicini. *Solid State Physics*. Second Edition. Academic Press, 2014.

[6] J. E. Hirsch. "Two-dimensional Hubbard model: Numerical simulation study". In: *Phys. Rev. B* 31 (7 Apr. 1985), pp. 4403–4419. DOI: 10.1103/PhysRevB.31.4403. URL: https://link.aps.org/doi/10.1103/PhysRevB.31.4403.

[7] Robin Scholle et al. "Comprehensive mean-field analysis of magnetic and charge orders in the two-dimensional Hubbard model". In: *Phys. Rev. B* 108 (3 July 2023), p. 035139. DOI: 10.1103/PhysRevB.108.035139. URL: https://link.aps.org/doi/10.1103/PhysRevB.108.035139.